6-14-2023

Material design and performance of carbon monoxide-fueled solid oxide fuel cells: A review

Wei Zhang
Michigan Technological University, weizhang@mtu.edu

Yun Hang Hu
Michigan Technological University, yunhangh@mtu.edu

Received: 7 March 2023 | Revised: 25 May 2023 | Accepted: 31 May 2023

DOI: 10.1002/ese3.1502

REVIEW

Material design and performance of carbon monoxide-fueled solid oxide fuel cells: A review

Wei Zhang | **Yun Hang Hu**

Department of Materials Science and Engineering, Michigan Technological University, Houghton, Michigan, USA

Correspondence
Yun Hang Hu, Department of Materials Science and Engineering, Michigan Technological University, Houghton, MI 49931, USA.
Email: yunhangh@mtu.edu

Abstract

Solid oxide fuel cells (SOFCs) are electrochemical energy conversion devices with fuel flexibility. Since carbon monoxide (CO) is a major product of SOFC anodes operating with hydrocarbon fuels, direct utilization of CO as a fuel is expected for more efficient operation of SOFCs. A review on CO-fueled SOFC technologies is imperative to promote research activities in this important field, but it has not been published. In this review, we summarize and comment on literatures in this field, with respect to (1) materials developed for three fundamental components (anode, cathode, and electrolyte), (2) power output and stabilization strategies, and (3) critical challenges and directions in the development of CO-fueled SOFCs.

KEYWORDS

carbon monoxide, electrochemical performances, materials development, scientific challenges, solid oxide fuel cells

1 | INTRODUCTION

Efficient energy devices are extremely important to solve energy and environmental issues.[1–5] Fuel cells are electrochemical devices that are capable of directly converting chemical fuels to electricity. Compared with the conventional heat engine that burns the fuels to produce heat energy for propelling the engine, the energy conversion of fuel cells is an "electrochemical process" with much higher efficiency.[6–8] A fuel cell consists of three essential components: anode, cathode, and electrolyte.[9–11] A typical operation mechanism of a fuel cell includes the three steps: (1) the oxidation of fuel on the anode to generate electrons; (2) the reduction of oxidant on the cathode by the electrons transported from the anode through an external circuit; (3) the transportation of as-produced ionic species (e.g., O^{2-}, H^{+}) through the electrolyte. Consequently, a continuous current can be generated as long as the fuel and the oxidant are supplied to the anode and the cathode, respectively. A graphical illustration of five classic types of fuel cells was shown in Figure 1, primarily classified by the state of the electrolyte, where the electrolyte type further determines the operating temperature of each fuel cell type.[8]

Alkaline fuel cells (AFCs), polymer electrolyte membrane fuel cells (PEMFCs), and phosphoric acid fuel cells (PAFCs) can operate at a relatively low-temperature range (≤200°C) using high-conducting liquid/polymer electrolytes with efficient ionic conduction.[12–14] However, precious metal-based catalysts (e.g., platinum) are required for PEMFCs and PAFCs to dissociate hydrogen/oxygen molecules on anode/cathode, leading to a high cost.[15,16] In contrast, since the electrolyte of AFCs transports OH^{-} instead of H^{+}, the utilization of low-cost catalysts (e.g., nickel) becomes possible for catalytic oxygen reduction, because oxygen

reduction kinetics is generally faster in an alkaline environment than in an acidic environment.[17] Nevertheless, AFCs suffer from a carbonation issue caused by the interaction between the electrolyte (KOH) and CO_2 (from air), forming a K_2CO_3 precipitate that blocks the pores of the cathode.[18]

Molten carbonate fuel cells (MCFCs) and solid oxide fuel cells (SOFCs) operate at relatively high temperatures (≥500°C).[19,20] MCFCs employ a molten carbonate composite as the electrolyte distributed in a porous, chemically stable medium. The high operating temperature of MCFCs enables the sufficient catalytic activity of electrodes even with nonprecious metal-based catalysts (e.g., Ni-based alloys/oxides). Besides, the molten electrolyte of MCFCs transports CO_3^{2-} (produced from O_2, CO_2, and e^- on the cathode), thus the CO_2-induced carbonation in AFCs is not an issue for MCFCs. However, insufficient corrosion resistance of steel-based components as interconnectors under the molten electrolyte condition could limit the lifetime of MCFCs.[21] Different from MCFCs, SOFCs employ a solid oxide as the ion-conducting electrolyte, which requires a high operating temperature to achieve fast ionic conduction in oxides and high electrode activity. Moreover, the all-solid configuration can reduce the possibility of corrosion faced by MCFCs and increase the variety of architectures (e.g., flat plates and rolled tubes) to fit versatile functions.[22] Notably, as breakthroughs in this area, semiconductor electrolyte-based fuel cells,[23] protonic ceramic fuel cells,[24,25] and carbonate-superstructured solid fuel cells[26] were recently developed. These advanced designs achieved excellent power output on a variety of fuels, leading to promising research frontiers.

SOFCs possess a high flexibility for fuels (such as hydrogen, hydrocarbons, and CO).[27–29] Many excellent reviews have been published on SOFCs operated with hydrogen and hydrocarbon fuels.[20,30–36] However, so far, there has not been an article to review the progress of SOFCs operated with CO fuel. This situation stimulated us to write this review article on the progress of CO-fueled SOFCs with an emphasis on materials and cell performances.

2 | BASIC REQUIREMENTS OF MATERIALS FOR CO-FUELED SOFCS

As the core component in CO-fueled SOFCs, the solid-oxide electrolyte, which is an oxide ionic transport medium, must meet the following requirements[37–40]: (1) It possesses sufficient oxide ionic conductivity and negligible electronic conductivity, ensuring that electrons produced on anode can be separated and continuously transported through the external circuit to generate an effective current/power output. (2) It maintains a high gas tightness as a membrane to separate fuel and oxidant on its two sides, preventing the direct combustion of the fuel. (3) Its thermal expansion coefficient is comparable to those of two electrodes to avoid cracking and peeling of cell components. (4) It possesses excellent physical and chemical stability in CO (fuel), CO_2 (major product from anode), and air/O_2 (oxidant) atmospheres at high temperatures to achieve a high cell durability.

Materials for CO-fueled SOFC electrodes (anode and cathode) should possess proper thermal expansion coefficients, high stability, and low cost. Furthermore, some rules were specially developed for electrode materials compared with those for the electrolyte[41–44]: (1) Materials of anode and cathode must be active for catalytic oxidation of CO and reduction of O_2, respectively. (2) Appropriate porosities are required for efficient diffusion of gas in electrode layers to ensure the interaction between gas molecules and catalysts. (3) High electronic conductivity of electrodes is critical for exporting/importing electrons constantly. (4) Excellent oxide ionic conductivity can extend the electrochemically active region in electrodes. (5) Particularly, modern

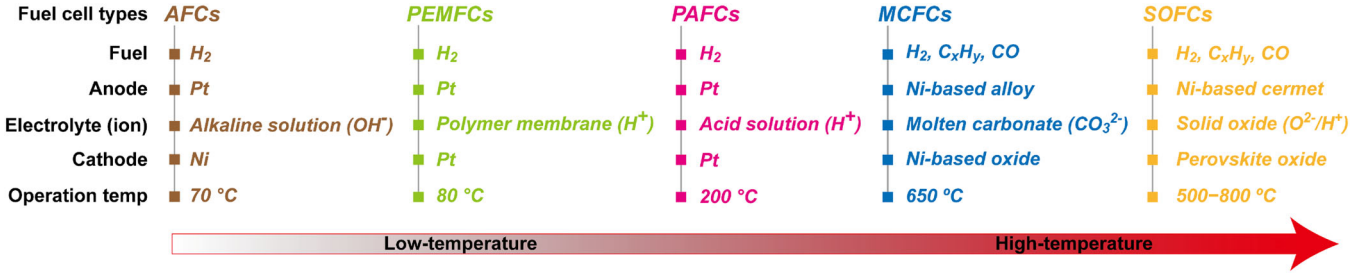

FIGURE 1 Five basic types of fuel cells showing their typical fuels, anode materials, electrolyte types (along with ionic species in the electrolyte), cathode materials, and operating temperatures. AFCs, alkaline fuel cells; CO, carbon monoxide; MCFCs, molten carbonate fuel cells; PAFCs, phosphoric acid fuel cells; PEMFCs, polymer electrolyte membrane fuel cells; SOFCs, solid oxide fuel cells.

planar SOFCs generally possess a gradient-structured configuration with a thick load-bearing anode to achieve sufficient mechanical strength.[45–47]

The SOFC technology offers much more competitive opportunities than low-temperature-type fuel cells (to AFCs, PEMFCs, and PAFCs) with respect to its flexible fuel options because the relatively high operating temperature of SOFCs enables the efficient catalytic activation of various fuels on the anode (such as H_2, hydrocarbons, CO, coal, and biomass).[48–52] Because H_2 and CO are intermediate products from the catalytic activation of hydrocarbon fuel during SOFC operation,[53,54] the direct utilization of CO as a fuel would enhance the cell efficiency with a simple anode reaction, namely, CO is oxidized on the anode with the generation of CO_2 and electrons (Equation 1)

$$CO+O^{2-} \rightarrow CO_2 + 2e^{-}. \quad (1)$$

The main challenge for the development of CO-fueled SOFCs is the low coking tolerance of Ni-based anodes to CO.[55–60]

3 | MATERIAL DEVELOPMENT OF CO-FUELED SOFCS

3.1 | Anode materials

Ni-based cermets could be used as anodes for SOFCs with CO fuel, but these anodes with CO showed significantly lower performance compared to that with H_2 fuel.[56,60] The incorporation of an appropriate amount of water into CO fuel is generally employed because H_2 can be produced from the water gas shift reaction[58]

$$CO+H_2O \rightarrow CO_2 + H_2. \quad (2)$$

To increase anode stability, various strategies were employed to modify its materials. As reported, Fe and MgO could stabilize the Ni-yttria-stabilized zirconia (Ni-YSZ) electrode for CO-fueled SOFCs.[58] In the elaborate anode composition of ($Ni_{0.75}Fe_{0.25}$-5%MgO)-YSZ, Ni/Fe would be an excellent catalyst, while MgO could enhance the structural stability of the anode via neutralizing the stress produced by carbon fiber growth. It was found that the composite anode with MgO showed a relatively "clean" surface after its operation in CO, whereas more small clusters were produced in the Ni-YSZ anode, blocking its pores (Figure 2). Besides, the wet CO (3% H_2O humidified) exhibited a lower power density than the dry CO, which might be due to the water-induced destabilization of MgO.[61]

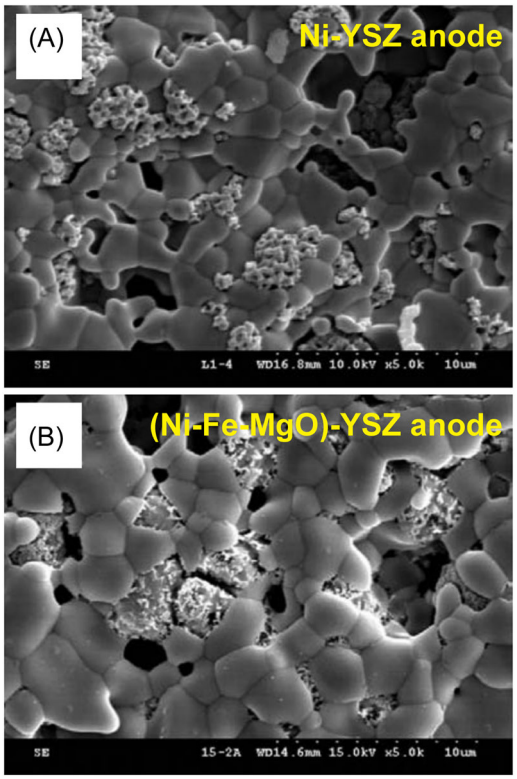

FIGURE 2 Scanning electron microscope images of (A) Ni-yttria-stabilized zirconia (Ni-YSZ) anode and (B) ($Ni_{0.75}Fe_{0.25}$-5% MgO)-YSZ anode after fuel cell test with carbon monoxide (CO) fuel. Reprinted with permission from Liu et al.[58]

Cu-CeO_2-YSZ anode was fabricated by modifying conventional Ni-YSZ anode for CO-fueled SOFCs.[56] In the electrode, CeO_2 and Cu acted as a catalyst and as an electronic conductor, respectively, while the YSZ played the role of oxide-ion conductor. To evaluate the effect of CO_2 on the electrode performance, 50% CO_2-diluted CO was fueled for the cell with Cu-CeO_2-YSZ anode, exhibiting an open-circuit voltage (OCV) of 0.97 V at 700°C, which is significantly lower than that (1.2 V) with pure CO fuel. Furthermore, the CO_2-induced reduction in OCV decreased the current density by 27% at 700°C. However, the *I–V* (current–voltage) curve for pure CO fuel is parallel to that for CO_2-diluted CO fuel, indicating that the introduction of CO_2 did not change the oxidation activation energy of CO on the Cu-CeO_2-YSZ anode. A similar CO_2 effect was observed for a conventional Ni-YSZ anode, namely, when 56% CO_2-diluted CO fuel replaced pure CO fuel, OCV decreased from 1 to 0.89V, whereas the corresponding current density was reduced by ~60% at 800°C.[55] However, the introduction of CO_2 into CO fuel increased the activation energy of CO oxidation on the Ni-YSZ anode, reflected by nonparallel *I–V* curves for the CO_2-diluted CO fuel and the pure CO fuel.[62,63] Therefore, one can conclude that the replacement of Ni in

the Ni-YSZ electrode by Cu/CeO_2 can inhibit the CO_2-induced deactivation of CO oxidation.

$La_{0.6}Sr_{0.4}Fe_{0.9}Nb_{0.1}O_{3-\delta}$ (LSFNb) perovskite was exploited both as an anode and a cathode to fabricate a symmetrical SOFC fueled with CO.[60] This material was derived from the classic lanthanum ferrite cathode family by doping a small amount of Nb to the B site of the ABO_3-structured perovskite.[64] The stronger Nb–O bond than Fe–O bond greatly contributed to its structural stability,[65] while the Fe-based B site of perovskite enabled appreciable conductivities in both reducing and oxidizing atmospheres.[66,67] Such a symmetrical cell configuration may contribute to enhanced tolerance to poisoning,[68,69] which can be readily achieved by a "switch" of fuel and oxidant, because poisonous elements (e.g., carbon, sulfur) grown on the former anode can be eliminated under oxidizing conditions (now as cathode) by forming waste gases. A series of chemically stable metal cations (e.g., Cr, Ti, Mo) could be considered as the alternative to Nb on the B site of perovskite to further stabilize its structure.[70–72] However, the catalytic mechanism of the CO fuel on an LSFNb perovskite anode needs to be revealed with future efforts.

3.2 | Cathode materials

The attempt on cathodes of CO-fueled SOFCs has mainly focused on three perovskite families: lanthanum manganite, lanthanum cobaltite, and lanthanum ferrite.[55–60] As widely demonstrated in "conventional" SOFCs operated with H_2 fuel,[73] these materials are excellent mixed ionic–electronic conductors (MIECs) allowing the transportation of both O^{2-} and e^-. Direct utilization of the developed MIECs is technologically feasible for CO-fueled SOFCs. Furthermore, proton transport is a preferable property for H_2-fueled SOFC cathodes if the electrolyte is a proton conductor. Proton transport in cathodes is helpful for extending the electrochemically active region.[74–78] In contrast, proton transport is not required for the cathode of CO-fueled SOFCs, namely, the triple-conducting (i.e., H^+, O^{2-}, and e^-) cathode developed for proton-conducting electrolyte-based SOFCs with H_2 fuel is no longer a necessity for the cell with CO fuel.

In general, the A-site cations of these perovskite-structured (ABO_3) MIECs consist of rare/alkaline earth elements (e.g., La, Sr, Ca, Ba), where the A^{3+} ion can be partially replaced by a dopant (e.g., A'^{2+}) at the A-site. Furthermore, the B sites typically contain reducible transition metal elements (e.g., Mn, Fe, Co, Ni), thus the B site cation can easily be reduced (e.g., B^{3+} to B^{2+}). With these strategies, considerable oxide-ion conductivity can be generated by the formation of oxygen vacancies, leading to an $A_{1-x}A'_xBO_{3-\delta}$ structure. Particularly, the B site cation also acts as an efficient catalyst for oxygen reduction.[79]

The typical SOFC cathode material, Sr-doped lanthanum manganite (LSM), was intensively employed in CO-fueled SOFCs,[57–59] taking advantage of its excellent electronic conductivity and high activity. A common approach to enhance its oxide-ion conductivity extrinsically is to mix the LSM with corresponding electrolyte material to form a composite cathode. For example, a mixed LSM-YSZ cathode (named as "functional layer") was coated on the YSZ electrolyte to achieve high compatibility.[58]

A compositionally graded cathode with an interlayer (between the "function layer" and the "current collector") would be useful to achieve better sinterability. For example, LSM-LSC (LaSrCo-oxide) mixture was deposited between the LSM-YSZ functional layer and a pure LSC current conducting layer (i.e., "LSM-YSZ|LSM-LSC|LSC"; Figure 3).[57] Herein, Co was used primarily due to its superiority in electronic conductivity over others.[80] Furthermore, the interlayer can avoid the direct reaction between LSC and YSZ, which could generate an unwanted insulating $La_2Zr_2O_7$ phase, enabling the use of a high sintering temperature for better sinterability.[81]

Fe-containing cathodes at the B site of ABO_3 perovskite were also explored for CO-fueled SOFCs. Using Fe at the B site of the ABO_3-type perovskite can generate the highest electronic conductivity compared with using other analogues (e.g., Al, Cr, Mn, Co, and Ga). The thermal expansion coefficient of Fe-containing

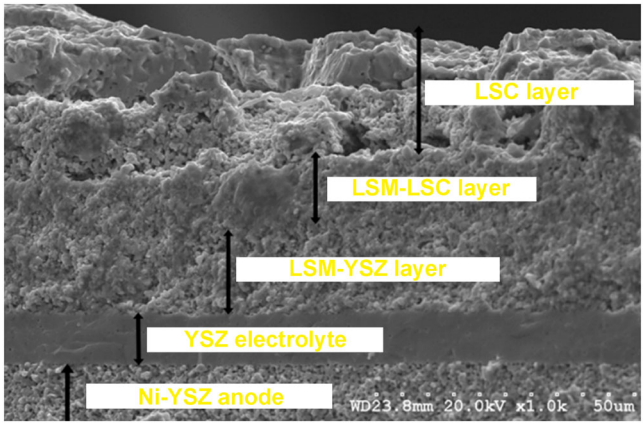

FIGURE 3 Cross-sectional scanning electron microscope image of the compositionally graded "LSM-YSZ|LSM-LSC|LSC" cathode. Sr-doped lanthanum manganite-yttria-stabilized zirconia (LSM-YSZ) is the catalytic functional layer; LaSrCo-oxide (LSC) is the current collector; LSM-LSC separates LSM-YSZ and LSC. Reprinted with permission from Homel et al.[57]

composition is also closer to the YSZ electrolyte than others, leading to better sinterability.[82] As a highlight, a two-step strategy was designed for the preparation of the Fe-containing composite cathode of LaSrFe-oxide (LSF) with YSZ.[56] The first step was to make a porous "YSZ cathode" layer on a dense YSZ electrolyte substrate using the tape casting process. Pore formers of graphite and polymethylmethacrylate were used in the "YSZ cathode" slurry, and a fine porous structure can be readily formed after drying and sintering. As the second step, the LSF was added into the as-prepared "YSZ cathode" framework to form the LSF-YSZ composite, achieved by impregnating the solutions of La/Sr/Fe nitrates. The two-step strategy can allow individual sintering temperatures, namely, the porous YSZ was sintered at a higher temperature (1550°C) together with the YSZ electrolyte, while the impregnated active composition of LSF was sintered at a relatively low temperature (850°C). This could eliminate the unwanted chemical reactions between LSF and YSZ.[81]

3.3 | Electrolyte materials

Electrolytes provide the function for oxide ion (O^{2-}) transfer from the cathode to the anode in CO-fueled SOFCs. Oxide-ion conducting electrolyte materials can be designed by a "doping" strategy.[83] A typical example is the renowned YSZ electrolyte with a fluorite crystal structure.[84] It is based on a ZrO_2 lattice with face-centered cubic-distributed Zr^{4+} sites and a simple cubic arrangement of O^{2-} sites. If a Zr^{4+} site (named as host cation) is replaced by a lower-valent cation (e.g., Y^{3+}, named as dopant cation), the missing charge would be balanced by forming oxygen vacancies. Continuous space is then generated for mobile O^{2-} along these vacancies in the lattice of the Y-doped ZrO_2. This mechanism has enabled decent oxide-ion conductivity in the YSZ electrolyte (e.g., ~10^{-2} S cm^{-1} at ~700°C),[85,86] leading to its dominant applications in the high-temperature operation of CO-fueled SOFCs.[55–60]

In addition to the direct use of YSZ as the electrolyte, an attempt on improving its chemical compatibility with electrodes has also been conducted. It was found that inserting an additional $Ce_{0.8}Gd_{0.2}O_{2-\delta}$ (gadolinia-doped ceria, GDC) as a "buffer" layer could suppress the chemical reaction between the YSZ electrolyte and the LSFNb electrode.[60] Namely, the YSZ electrolyte layer and GDC buffer layer were firstly cosintered at 1300°C for 3 h. Then, the LSFNb electrode was coated on the surface of GDC and sintered at 1000°C, obtaining a "YSZ (200 μm)|GDC (4 μm)|LSFNb (20 μm)" three-layer structure (Figure 4A). The higher sintering temperature in the first step ensured the densification of the YSZ electrolyte, while the lower sintering temperature in the second step was enough for retaining the LSFNb on GDC and avoiding any temperature-induced reaction. Notably, although GDC itself is an intrinsic oxide-ion conductor, it may be converted to an electronic conductor during fuel cell operation because of the facile reduction of Ce^{4+} to Ce^{3+} in a reducing atmosphere.[77,87] The oxide-ion conducting role of the YSZ electrolyte would not be affected by the GDC buffer layer.

The well-known $La_{0.8}Sr_{0.2}Ga_{0.83}Mg_{0.17}O_{3-\delta}$ (Sr-Mg-doped $LaGaO_3$, LSGM) electrolyte was also employed for SOFCs operated with CO fuel. The lanthanum gallate-based perovskites have shown higher ionic conductivity (~10^{-1} S cm^{-1} at 700°C) compared with YSZ.[88] However, the LSGM electrolyte suffers from some issues (including the formation of impurities, such as $LaSrGa_3O_7$ and

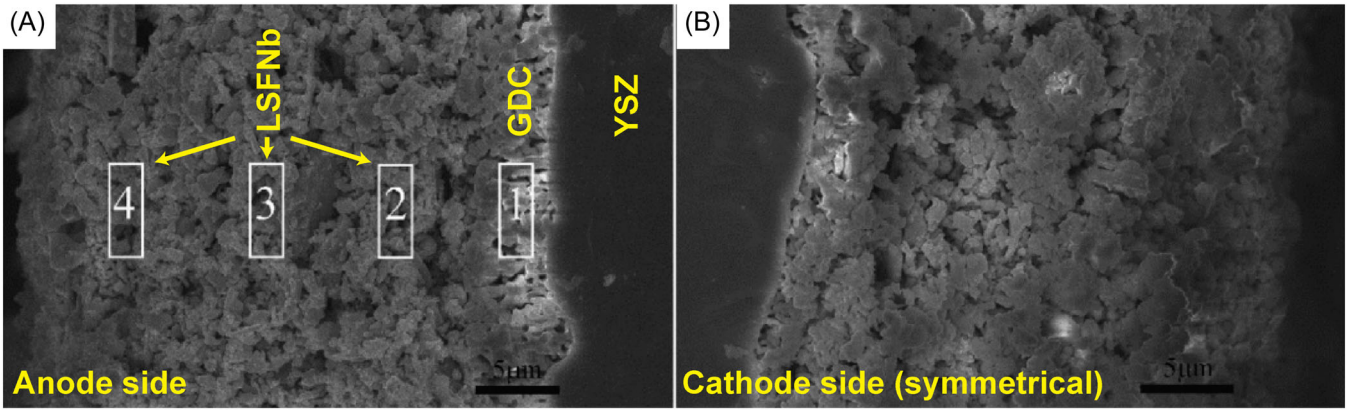

FIGURE 4 Cross-sectional scanning electron microscope images of the symmetrical "LSFNb|GDC|YSZ|GDC|LSFNb" structure. (A) Anode side shows the dense yttria-stabilized zirconia (YSZ) electrolyte, GDC buffer layer, and LSFNb electrode. Energy-dispersive X-ray spectroscopy elemental analysis was performed on the numbered regions to distinguish GDC and LSFNb. (B) Symmetrical cathode side. GDC, gadolinia-doped ceria; LSFNb, $La_{0.6}Sr_{0.4}Fe_{0.9}Nb_{0.1}O_{3-\delta}$. Reprinted with permission from Bian et al.[60]

$LaSrGaO_4$) due to its high reactivity with nickel-containing electrodes.[89–91] One possible solution is to develop nickel-free electrodes to mitigate the reaction between the LSGM and electrode materials.[92,93] Besides, it was reported that introducing a certain amount of Fe_2O_3 to NiO could improve the chemical compatibility between LSGM and NiO.[94] With respect to the specific application of LSGM electrolyte to the CO-fueled SOFCs, an integrated strategy was explored, namely, Fe-based Ni-free symmetrical electrodes were used on both sides of the LSGM electrolyte, exhibiting excellent cell performance.[60]

4 | ELECTROCHEMICAL PERFORMANCES OF CO-FUELED SOFCS

Performances with CO fuel were evaluated for SOFCs with various electrolytes and electrodes. As shown in Figure 5 and Table 1, one can see that research efforts on CO-fueled SOFCs were mainly focused on the high-temperature (HT) region (≥800°C). This happened because this high-temperature range can ensure large ionic conduction in electrolytes and high catalytic activity in electrodes, boosting cell performance. Furthermore, the best CO-fueled cells reached excellent power densities of ~700 mW cm^{-2} at 800°C. Compared with "conventional" YSZ-based SOFCs using hydrogen and hydrocarbon fuels,[24] the optimized CO-fueled devices reached approximately half of the best performance of hydrogen/hydrocarbon-fueled SOFCs (~1400 mW cm^{-2} at 800°C). From the perspective of electrode materials, Co/Fe-based electrodes showed the best performance at 700–850°C. Although the YSZ played a dominant role as the electrolyte (occupied 91% of data), the utilization of LSGM electrolyte has identified a promising research direction, with the best performance of 707 mW cm^{-2} at 850°C. Nevertheless, reducing the operating temperature of SOFCs to the intermediate-temperature (IT) range (about 500–700°C) is a current research trend,[8,95,96] which can provide many benefits, including the decreased cost of components, faster startup process, mitigated thermal diffusion, enhanced operational stability, and simple system architecture. Therefore, there are promising opportunities to develop CO-fueled SOFCs for operation at lower temperatures (down to 500°C).

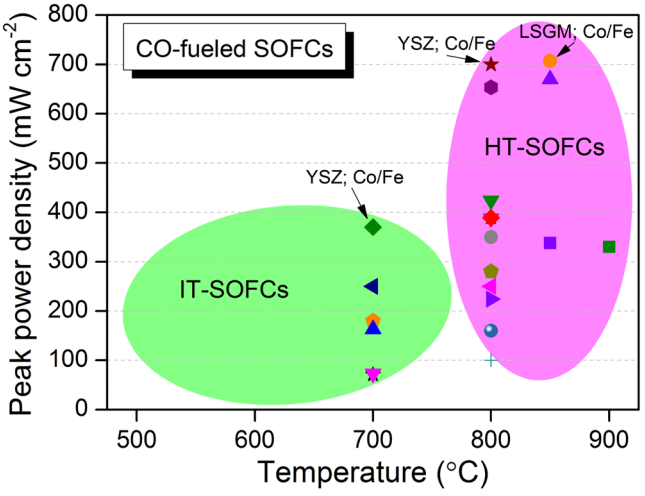

FIGURE 5 Summary of peak power densities of carbon monoxide (CO)-fueled solid oxide fuel cells (SOFCs) reported in the literatures. Twenty-two data points were collected in this figure, which were classified by operating temperature ranges. The as-used materials (electrolyte; electrode) for the best-performing cells were annotated. More detailed information was provided in Table 1. HT, high temperature; IT, intermediate temperature.

It is essential for CO-fueled SOFCs to be stable during a long-term operation. So far, the best reported CO-fueled SOFC is the tubular cell fabricated with Ni-YSZ anode (0.8–1.0 mm thickness), YSZ electrolyte (8–10 μm thick membrane), and LSM-YSZ cathode (20 μm thick).[57] The cell remained almost unchanged with a power output of ~280 mW cm^{-2} at 850°C for a long-term operation of 375 h (Figure 6A), leading to a very low degradation rate below 0.1% per 1000 h. Notably, there was a quick drop at the initial stage in the first 24 h (Figure 6A). The initial degradation might be caused by strong chemical reaction-induced interfacial disturbance at the "electrolyte/electrode" or "electrode/current collector" interfaces. However, the removal of deposited carbon on the Ni-based anode may also play a significant role. First, under open-circuit conditions (i.e., without current output), the formation of carbon deposition on Ni-based anode is thermodynamically preferable at 850°C via the disproportionation of CO[57]

$$2CO \rightarrow CO_2 + C. \quad (3)$$

The mechanism of CO disproportionation to carbon on the Ni-based anode was proposed as follows[97]:

$$CO + * \rightarrow CO*, \quad (4)$$

$$CO* + * \rightarrow C*+O*, \quad (5)$$

$$CO* + O* \rightarrow CO_2 + 2*, \quad (6)$$

$$C* \rightarrow C_{Ni,f} + *, \quad (7)$$

where * represents a Ni surface site and $C_{Ni,f}$ the as-formed carbon on a Ni site. Second, under operating

TABLE 1 Summary of CO-fueled SOFCs listing the as-employed materials, fuel composition, fuel utilization, test temperature, PPD, power density measured at an operating voltage of 0.7 V (estimated from reported *I–V* curves), stability, reference, and published year.

Anode	Cathode	Electrolyte	Fuel	Fuel utilization (%)	Temperature (°C)	PPD (mW cm^{-2})	Power density at 0.7 V (mW cm^{-2})	Stability	Reference	Year
Ni-YSZ	LSC-SDC	YSZ/SDC	Dry CO	N/A	800	700	600	N/A	[55]	2003
Ni-YSZ	LSC-SDC	YSZ/SDC	44% CO–56% CO_2	N/A	800	280	210	N/A	[55]	2003
Ni-YSZ	LSC-SDC	YSZ/SDC	32% CO–68% CO_2	N/A	800	160	110	N/A	[55]	2003
Ni-YSZ	LSC-SDC	YSZ/SDC	18% CO–82% CO_2	N/A	800	100	50	N/A	[55]	2003
Ni-YSZ	LSF-YSZ	YSZ	Dry CO	N/A	700	73	50	N/A	[56]	2005
Cu-Co-CeO_2-YSZ	LSF-YSZ	YSZ	Dry CO	N/A	700	370	350	N/A	[56]	2005
Ni-YSZ	(LSM-YSZ)/(LSM-LSC)/LSC	YSZ	Dry CO	20	850	670	600	375 h	[57]	2010
Ni-YSZ	(LSM-YSZ)/(LSM-LSC)/LSC	YSZ	50% CO–50% CO_2	20–50	900	330	290	N/A	[57]	2010
Ni-YSZ	(LSM-YSZ)/(LSM-LSC)/LSC	YSZ	50% CO–50% CO_2	20–50	800	250	220	N/A	[57]	2010
Ni-YSZ	(LSM-YSZ)/LSC	YSZ	95% CO–5% CO_2	40–60	800	224 (50-cell stack)	N/A	N/A	[57]	2010
Ni-YSZ	LSM-YSZ/LSM	YSZ	Dry CO	N/A	800	390	330	<5 h	[58]	2012
Ni-YSZ	LSM-YSZ/LSM	YSZ	Wet CO	N/A	800	350	310	10 h	[58]	2012
(Ni-Fe-MgO)-YSZ	LSM-YSZ/LSM	YSZ	Dry CO	N/A	800	424	380	40 h	[58]	2012
(Ni-Fe-MgO)-YSZ	LSM-YSZ/LSM	YSZ	Wet CO	N/A	800	388	330	40 h	[58]	2012
(Ni-Fe-MgO)-YSZ	LSM-YSZ/LSM	YSZ	Wet CO	N/A	800	389 (two-cell stack)	320	60 h	[58]	2012
(Ni-Fe-MgO)-YSZ	LSM-YSZ/LSM	YSZ	Wet CO	N/A	700	163 (two-cell stack)	140	30 h	[58]	2012
Ni-YSZ	YSZ-LSM	YSZ	Dry CO	N/A	800	653.6	525	N/A	[59]	2013
Ni-YSZ	YSZ-LSM	YSZ	Dry CO	N/A	700	250	175	N/A	[59]	2013

(Continues)

TABLE 1 (Continued)

Anode	Cathode	Electrolyte	Fuel	Fuel utilization (%)	Temperature (°C)	PPD (mW cm^{-2})	Power density at 0.7 V (mW cm^{-2})	Stability	Reference	Year
LSFNb	LSFNb	GDC/YSZ/GDC	Dry CO	N/A	850	338	300	90 h (@800°C)	[60]	2019
LSFNb	LSFNb	GDC/YSZ/GDC	Dry CO	N/A	700	71	60	N/A	[60]	2019
LSFNb	LSFNb	LSGM	Dry CO	N/A	850	707	600	N/A	[60]	2019
LSFNb	LSFNb	LSGM	Dry CO	N/A	700	180	170	N/A	[60]	2019

Abbreviations: CO, carbon monoxide; GDC, gadolinia-doped ceria; LSC, LaSrCo-oxide; LSF, lanthanum strontium ferrite; LSFNb, $La_{0.6}Sr_{0.4}Fe_{0.9}Nb_{0.1}O_{3-\delta}$; LSGM, Sr-Mg-doped $LaGaO_3$; LSM, Sr-doped lanthanum manganite; N/A, not available; PPD, peak power density; SDC, samaria-doped ceria; SOFC, solid oxide fuel cell; YSZ, yttria-stabilized zirconia.

conditions with a fixed current output (i.e., during discharge), O^{2-} ions generated on the cathode can be transported to the anode. This could be a possible reason for the removal of carbon on the anode by the following reaction:

$$C + 2O^{2-} \rightarrow CO_2 + 4e^{-}. \quad (8)$$

Consequently, the cell showed a stable performance after the first 24 h.

The stability of YSZ-based SOFCs with symmetrical LSFNb electrodes (as both anode and cathode) was examined with CO fuel.[60] A relatively stable power output of 140−150 mW cm^{-2} was recorded at 800°C for 90 h (Figure 6B). The degradation rate of cell voltage is ~0.14 mV h^{-1}, which is equivalent to a degradation rate of 18.7% per 1000 h. This is inferior to the stability (0.1% per 1000) of the asymmetrical YSZ-based SOFC with Ni-YSZ anode and LSM-YSZ cathode.[57]

The effects of Fe/Mg (in anode) and water (in fuel) on cell stability were also assessed for CO-fueled YSZ-based SOFCs.[58] Two cells with conventional Ni-YSZ anode and ($Ni_{0.75}Fe_{0.25}$-5%MgO)-YSZ anode were tested under dry/wet CO-fueled conditions (Figure 6C). When a fixed current output of 83 mA cm^{-2} was applied for the stability test at 800°C, the stable performance of the cell with Ni-YSZ anode remained for only 10 h with wet CO fuel and 5 h with dry CO fuel. This indicates that CO-fueled YSZ-based SOFCs with Ni-YSZ anode possess poor stability and water in CO fuel can slightly improve cell stability. In contrast, the cell with ($Ni_{0.75}Fe_{0.25}$-5%MgO)-YSZ anode exhibited steady performance for 40 h using both dry and wet CO. Furthermore, a cell stack comprising two-cell units with the ($Ni_{0.75}Fe_{0.25}$-5% MgO)-YSZ anode exhibited good stability with wet CO fuel for 90 h at 800/700°C (Figure 6D). This clearly demonstrates that the Fe/Mg in the Ni-YSZ anode could play an important role in inhibiting the degradation of cell performance.

5 | SUMMARY AND OUTLOOK

SOFCs operated with CO fuel have shown inspiring electrochemical performances at a high-temperature range (700−850°C), achieving excellent power densities up to ~700 mW cm^{-2} and a stable operation for nearly 400 h. The classic cell with the "Ni-YSZ anode| YSZ electrolyte|LSM-YSZ cathode" configuration was improved by developing electrolyte and electrode materials for its operation with CO fuel. Although YSZ dominates the electrolyte, the LSGM has shown its potential as an alternative to YSZ. Fe/Co/Cu- and

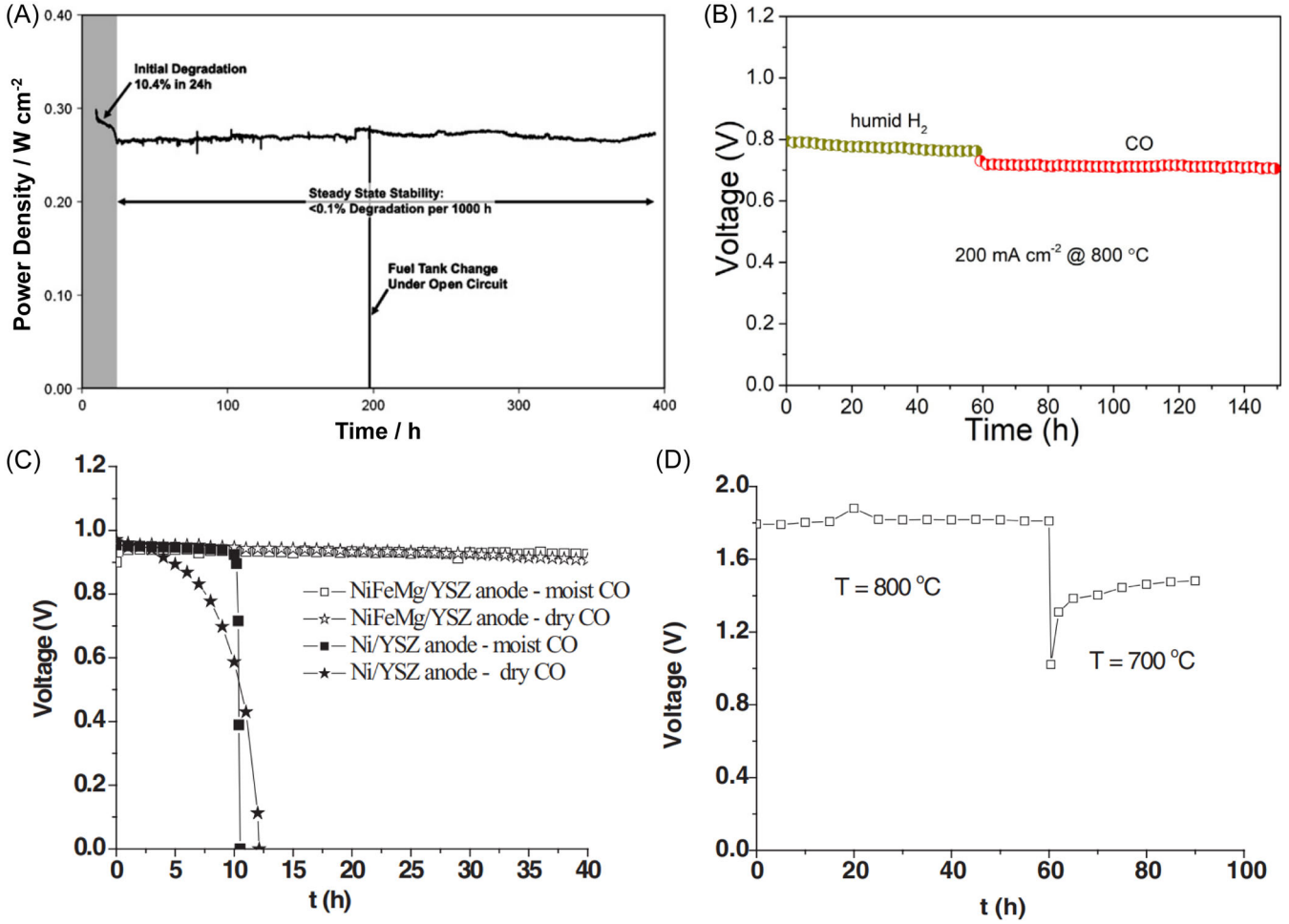

FIGURE 6 Stability of carbon monoxide (CO)-fueled solid oxide fuel cells (SOFCs): (A) SOFC with Ni-yttria-stabilized zirconia (Ni-YSZ) anode, YSZ electrolyte, and Sr-doped lanthanum manganite (LSM)-YSZ cathode. Reprinted with permission from Homel et al.[57] (B) SOFC with YSZ electrolyte and symmetrical $La_{0.6}Sr_{0.4}Fe_{0.9}Nb_{0.1}O_{3-\delta}$ (LSFNb) electrodes. Reprinted with permission from Bian et al.[60] (C) SOFCs with YSZ electrolyte, LSM-YSZ cathode, and fabricated with different anodes (Ni-YSZ and Ni-Fe-MgO-YSZ). (D) SOFC stack comprising two-cell units with the Ni-Fe-MgO-YSZ anode. Reprinted with permission from Liu et al.[58]

MgO-modified Ni-YSZ anodes exhibited excellent electrocatalytic activities and inhibited carbon deposition, leading to competitive power output and good stability. The combination of chemically stable oxides (e.g., CaO, TiO_2, SiO_2, and Al_2O_3) with Ni-based anodes deserves more attention to further enhance the structural strength of anodes under carbon-containing conditions. Improvements in cathodes have been focused on the replacement of LSM by Co/Fe-doped perovskite oxides for efficient oxygen reduction and electronic conduction. Furthermore, the multi-layered design of cathode structure would be helpful, such as the introduction of an "interlayer", to avoid side reactions at high sintering temperatures.

The CO-fueled SOFC is still in its infant stage, and intensive efforts are required for its development. Compared with SOFCs with H_2 fuel, the CO-fueled SOFCs exhibited worse performance mainly due to the slower oxidation of CO (to CO_2) than H_2 (to H_2O). For the enhanced performance of CO-fueled SOFCs, the higher oxide ionic conductivity of electrolytes is required to increase oxide ionic concentration at the anode and thus accelerate CO oxidation. Although various doped metal oxides were explored as oxide ionic conductive electrolytes for SOFCs,[98–100] new strategies would be employed to develop efficient electrolytes with high oxide ionic conductivity for CO-fueled SOFCs. For example, as recently reported,[26] in situ generation of superstructured carbonate in the porous samarium-doped ceria layer created a unique electrolyte with ultrahigh oxygen ionic conductivity. This finding deserves to be applied to the development of CO-fueled SOFCs.

Although the influence of coking on anodes was widely investigated, the complete inhibition of carbon deposition in CO-fueled SOFCs is still a challenge.[97,101–107] This will inspire more efforts to develop

efficient anode catalysts by inhibiting coking. The solid solution formation of Ni and MgO exhibited excellent performance for inhibiting carbon deposition.[108,109] The combination of Cu and Ni in an alloy achieved high catalytic activity and stability for CH_4-fueled SOFCs.[110] Those materials would be explored as anode catalysts for CO-fueled SOFCs. Furthermore, the symmetrical SOFC cell with LSFNb electrodes showed improved performance with CO fuel, which would provide another direction to achieve stable operation of CO-fueled SOFCs. This is because the carbon deposition can be efficiently removed by a simple "reverse" operation (namely, switching the fuel and oxidant).

The interfacial compatibility between different cell components needs to be improved for avoiding interdiffusion and direct reaction between cell components, which will promote the design of proper interlayers.[111,112] Furthermore, the formation of secondary phases at the electrolyte/electrode interface is mainly induced by the enhanced migration of cations at high temperatures.[113] Thus, addressing the interfacial issue strongly couples with the development of electrolyte materials that can operate at a reduced temperature, inspiring efforts to develop efficient CO-fueled SOFCs operating in a practical intermediate temperature range (e.g., 500−600°C).

ACKNOWLEDGMENTS

This work was partially supported by US National Science Foundation (CMMI-1661699).

CONFLICT OF INTEREST STATEMENT

The authors declare no conflict of interest.

ORCID

Yun Hang Hu http://orcid.org/0000-0002-5358-8667

REFERENCES

1. Wei W, Hu B, Jin F, et al. Potassium-chemical synthesis of 3D graphene from CO_2 and its excellent performance in HTM-free perovskite solar cells. *J Mater Chem A*. 2017;5(17):7749-7752.
2. Chang L, Hu YH. Breakthroughs in designing commercial-level mass-loading graphene electrodes for electrochemical double-layer capacitors. *Matter*. 2019;1(3):596-620.
3. Chang L, Sun Z, Hu YH. 1T phase transition metal dichalcogenides for hydrogen evolution reaction. *Electrochem Energy Rev*. 2021;4:194-218.
4. Chang L, Chen S, Fei Y, Stacchiola DJ, Hu YH. Superstructured $NiMoO_4$@$CoMoO_4$ core-shell nanofibers for supercapacitors with ultrahigh areal capacitance. *Proc Natl Acad Sci USA*. 2023;120(12):e2219950120.
5. Fang S, Lyu X, Tong T, et al. Turning dead leaves into an active multifunctional material as evaporator, photocatalyst, and bioplastic. *Nat Commun*. 2023;14(1):1203.
6. Dokiya M. SOFC system and technology. *Solid State Ionics*. 2002;152-153:383-392.
7. Blum L, Meulenberg WA, Nabielek H, Steinberger-Wilckens R. Worldwide SOFC technology overview and benchmark. *Int J Appl Ceram Technol*. 2005;2(6):482-492.
8. Brett DJL, Atkinson A, Brandon NP, Skinner SJ. Intermediate temperature solid oxide fuel cells. *Chem Soc Rev*. 2008;37(8):1568-1578.
9. Ivers-Tiffée E, Weber A, Herbstritt D. Materials and technologies for SOFC-components. *J Eur Ceram Soc*. 2001;21(10-11):1805-1811.
10. Dwivedi S. Solid oxide fuel cell: materials for anode, cathode and electrolyte. *Int J Hydrogen Energy*. 2020;45(44):23988-24013.
11. Hussain S, Yangping L. Review of solid oxide fuel cell materials: cathode, anode, and electrolyte. *Energy Trans*. 2020;4:113-126.
12. Stonehart P. Development of alloy electrocatalysts for phosphoric acid fuel cells (PAFC). *J Appl Electrochem*. 1992;22(11):995-1001.
13. Merle G, Wessling M, Nijmeijer K. Anion exchange membranes for alkaline fuel cells: a review. *J Membr Sci*. 2011;377(1-2):1-35.
14. Wang Y, Chen KS, Mishler J, Cho SC, Adroher XC. A review of polymer electrolyte membrane fuel cells: technology, applications, and needs on fundamental research. *Appl Energy*. 2011;88(4):981-1007.
15. Thompson SD, Jordan LR, Forsyth M. Platinum electrodeposition for polymer electrolyte membrane fuel cells. *Electrochim Acta*. 2001;46(10-11):1657-1663.
16. Sammes N, Bove R, Stahl K. Phosphoric acid fuel cells: fundamentals and applications. *Curr Opin Solid State Mater Sci*. 2004;8(5):372-378.
17. Lima FHB, Calegaro ML, Ticianelli EA. Investigations of the catalytic properties of manganese oxides for the oxygen reduction reaction in alkaline media. *J Electroanal Chem*. 2006;590(2):152-160.
18. Al-Saleh MA, Gültekin S, Al-Zakri AS, Celiker H. Effect of carbon dioxide on the performance of Ni/PTFE and Ag/PTFE electrodes in an alkaline fuel cell. *J Appl Electrochem*. 1994;24:575-580.
19. Dicks AL. Molten carbonate fuel cells. *Curr Opin Solid State Mater Sci*. 2004;8(5):379-383.
20. Mahato N, Banerjee A, Gupta A, Omar S, Balani K. Progress in material selection for solid oxide fuel cell technology: a review. *Prog Mater Sci*. 2015;72:141-337.
21. Biedenkopf P, Bischoff MM, Wochner T. Corrosion phenomena of alloys and electrode materials in molten carbonate fuel cells. *Mater Corros*. 2000;51(5):287-302.
22. Singhal S. Solid oxide fuel cells for stationary, mobile, and military applications. *Solid State Ionics*. 2002;152-153:405-410.
23. Zhu B, Yun S, Lund PD. Semiconductor-ionic materials could play an important role in advanced fuel-to-electricity conversion. *Int J Energy Res*. 2018;42(11):3413-3415.
24. Duan C, Tong J, Shang M, et al. Readily processed protonic ceramic fuel cells with high performance at low temperatures. *Science*. 2015;349(6254):1321-1326.

25. Duan C, Kee RJ, Zhu H, et al. Highly durable, coking and sulfur tolerant, fuel-flexible protonic ceramic fuel cells. *Nature*. 2018;557(7704):217-222.
26. Su H, Zhang W, Hu YH. Carbonate-superstructured solid fuel cells with hydrocarbon fuels. *Proc Natl Acad Sci USA*. 2022;119(41):e2208750119.
27. Eguchi K. Fuel flexibility in power generation by solid oxide fuel cells. *Solid State Ionics*. 2002;152-153:411-416.
28. Liu J, Madsen BD, Ji Z, Barnett SA. A fuel-flexible ceramic-based anode for solid oxide fuel cells. *Electrochem Solid-State Lett*. 2002;5(6):A122.
29. Yi Y, Rao AD, Brouwer J, Samuelsen GS. Fuel flexibility study of an integrated 25 kW SOFC reformer system. *J Power Sources*. 2005;144(1):67-76.
30. Mogensen M, Kammer K. Conversion of hydrocarbons in solid oxide fuel cells. *Annu Rev Mater Res*. 2003;33(1):321-331.
31. McIntosh S, Gorte RJ. Direct hydrocarbon solid oxide fuel cells. *Chem Rev*. 2004;104(10):4845-4866.
32. Ge XM, Chan SH, Liu QL, Sun Q. Solid oxide fuel cell anode materials for direct hydrocarbon utilization. *Adv Energy Mater*. 2012;2(10):1156-1181.
33. Da Silva FS, de Souza TM. Novel materials for solid oxide fuel cell technologies: a literature review. *Int J Hydrogen Energy*. 2017;42(41):26020-26036.
34. Abdalla AM, Hossain S, Azad AT, et al. Nanomaterials for solid oxide fuel cells: a review. *Renew Sustain Energy Rev*. 2018;82:353-368.
35. Su H, Hu YH. Progress in low-temperature solid oxide fuel cells with hydrocarbon fuels. *Chem Eng J*. 2020;402:126235.
36. Singh M, Zappa D, Comini E. Solid oxide fuel cell: decade of progress, future perspectives and challenges. *Int J Hydrogen Energy*. 2021;46(54):27643-27674.
37. Jaiswal N, Tanwar K, Suman R, Kumar D, Upadhyay S, Parkash O. A brief review on ceria based solid electrolytes for solid oxide fuel cells. *J Alloys Compd*. 2019;781:984-1005.
38. Wang F, Lyu Y, Chu D, Jin Z, Zhang G, Wang D. The electrolyte materials for SOFCs of low-intermediate temperature. *Mater Sci Technol*. 2019;35(13):1551-1562.
39. Shi H, Su C, Ran R, Cao J, Shao Z. Electrolyte materials for intermediate-temperature solid oxide fuel cells. *Prog Nat Sci Mater Int*. 2020;30(6):764-774.
40. Zakaria Z, Kamarudin SK. Advanced modification of Scandia-stabilized zirconia electrolytes for solid oxide fuel cells application—a review. *Int J Energy Res*. 2021;45(4):4871-4887.
41. Jiang SP. Nanoscale and nano-structured electrodes of solid oxide fuel cells by infiltration: advances and challenges. *Int J Hydrogen Energy*. 2012;37(1):449-470.
42. Hedayat N, Du Y, Ilkhani H. Pyrolyzable pore-formers for the porous-electrode formation in solid oxide fuel cells: a review. *Ceram Int*. 2018;44(5):4561-4576.
43. Afroze S, Karim A, Cheok Q, Eriksson S, Azad AK. Latest development of double perovskite electrode materials for solid oxide fuel cells: a review. *Front Energy*. 2019;13:770-797.
44. Cao T, Kwon O, Gorte RJ, Vohs JM. Metal exsolution to enhance the catalytic activity of electrodes in solid oxide fuel cells. *Nanomaterials*. 2020;10(12):2445.
45. Fashalameh KM, Sadeghian Z, Ebrahimi R. A high-performance planar anode-supported solid oxide fuel cell with hierarchical porous structure through slurry-based three-dimensional printing. *J Alloys Compd*. 2022;916:165406.
46. Ilbas M, Alemu MA, Cimen FM. Comparative performance analysis of a direct ammonia-fuelled anode supported flat tubular solid oxide fuel cell: a 3D numerical study. *Int J Hydrogen Energy*. 2022;47(5):3416-3428.
47. Pikalova E, Osinkin D, Kalinina E. Direct electrophoretic deposition and characterization of thin-film membranes based on doped $BaCeO_3$ and CeO_2 for anode-supported solid oxide fuel cells. *Membranes*. 2022;12(7):682.
48. Liu J. Operation of anode-supported solid oxide fuel cells on methane and natural gas. *Solid State Ionics*. 2003;158(1-2):11-16.
49. Inui Y, Urata A, Ito N, Nakajima T, Tanaka T. Performance simulation of planar SOFC using mixed hydrogen and carbon monoxide gases as fuel. *Energy Convers Manage*. 2006;47(13-14):1738-1747.
50. Sun C, Xie Z, Xia C, Li H, Chen L. Investigations of mesoporous CeO_2-Ru as a reforming catalyst layer for solid oxide fuel cells. *Electrochem Commun*. 2006;8(5):833-838.
51. Gür TM, Homel M, Virkar AV. High performance solid oxide fuel cell operating on dry gasified coal. *J Power Sources*. 2010;195(4):1085-1090.
52. Hibino T, Kobayashi K, Hitomi T. Biomass solid oxide fuel cell using solid weed waste as fuel. *Electrochim Acta*. 2021;388:138681.
53. Zhang W, Hu YH. CO-induced thermal decomposition of $LiNi_{0.8}Co_{0.15}Al_{0.05}O_2$. *Phys Lett A*. 2023;470:128774.
54. Zhang W, Hu YH. How stable is $LiNi_{0.8}Co_{0.15}Al_{0.05}O_2$ under high-temperature hydrocarbon ceramic fuel cell conditions? *Ceram Int*. 2023;49(2):3049-3057.
55. Jiang Y, Virkar AV. Fuel composition and diluent effect on gas transport and performance of anode-supported SOFCs. *J Electrochem Soc*. 2003;150(7):A942.
56. Costa-Nunes O, Gorte RJ, Vohs JM. Comparison of the performance of Cu–CeO_2–YSZ and Ni–YSZ composite SOFC anodes with H_2, CO, and syngas. *J Power Sources*. 2005;141(2):241-249.
57. Homel M, Gür TM, Koh JH, Virkar AV. Carbon monoxide-fueled solid oxide fuel cell. *J Power Sources*. 2010;195(19):6367-6372.
58. Liu Y, Bai Y, Liu J. Carbon monoxide fueled cone-shaped tubular solid oxide fuel cell with ($Ni_{0.75}Fe_{0.25}$-5%MgO)/YSZ anode. *J Electrochem Soc*. 2012;160(1):F13-F17.
59. Zhang H, Chen J, Zhang J. Performance analysis and parametric study of a solid oxide fuel cell fueled by carbon monoxide. *Int J Hydrogen Energy*. 2013;38(36):16354-16364.
60. Bian L, Wang L, Duan C, Cai C, Song X, An S. Co-free $La_{0.6}Sr_{0.4}Fe_{0.9}Nb_{0.1}O_{3-\delta}$ symmetric electrode for hydrogen and carbon monoxide solid oxide fuel cell. *Int J Hydrogen Energy*. 2019;44(60):32210-32218.
61. Furusawa T, Sato T, Saito M, et al. The evaluation of the stability of Ni/MgO catalysts for the gasification of lignin in supercritical water. *Appl Catal A*. 2007;327(2):300-310.

62. Yoon KJ, Zink P, Gopalan S, Pal UB. Polarization measurements on single-step Co-fired solid oxide fuel cells (SOFCs). *J Power Sources*. 2007;172(1):39-49.
63. Stoynov Z, Vladikova D, Burdin B, et al. Differential analysis of SOFC current–voltage characteristics. *Appl Energy*. 2018;228:1584-1590.
64. Zhang W, Hu YH. Recent progress in design and fabrication of SOFC cathodes for efficient catalytic oxygen reduction. *Catal Today*. 2023;409:71-86.
65. Shen P, Liu X, Wang H, Ding W. Niobium doping effects on performance of $BaCo_{0.7}Fe_{0.3-x}Nb_xO_{3-\delta}$ perovskite. *J Phys Chem*. 2010;114(50):22338-22345.
66. Liu X, Han D, Zhou Y, et al. Sc-substituted $La_{0.6}Sr_{0.4}FeO_{3-\delta}$ mixed conducting oxides as promising electrodes for symmetrical solid oxide fuel cells. *J Power Sources*. 2014;246:457-463.
67. Bian L, Duan C, Wang L, Zhu L, O'Hayre R, Chou K-C. Electrochemical performance and stability of $La_{0.5}Sr_{0.5}Fe_{0.9}Nb_{0.1}O_{3-\delta}$ symmetric electrode for solid oxide fuel cells. *J Power Sources*. 2018;399:398-405.
68. Ruiz-Morales JC, Canales-Vázquez J, Peña-Martínez J, López DM, Núñez P. On the simultaneous use of $La_{0.75}Sr_{0.25}Cr_{0.5}Mn_{0.5}O_{3-\delta}$ as both anode and cathode material with improved microstructure in solid oxide fuel cells. *Electrochim Acta*. 2006;52(1):278-284.
69. Ma Z, Sun C, Ma C, Wu H, Zhan Z, Chen L. Ni doped $La_{0.6}Sr_{0.4}FeO_{3-\delta}$ symmetrical electrode for solid oxide fuel cells. *Chin J Catal*. 2016;37(8):1347-1353.
70. Zhou Q, Yuan C, Han D, Luo T, Li J, Zhan Z. Evaluation of $LaSr_2Fe_2CrO_{9-\delta}$ as a potential electrode for symmetrical solid oxide fuel cells. *Electrochim Acta*. 2014;133:453-458.
71. Cao Z, Zhang Y, Miao J, et al. Titanium-substituted lanthanum strontium ferrite as a novel electrode material for symmetrical solid oxide fuel cell. *Int J Hydrogen Energy*. 2015;40(46):16572-16577.
72. Lu X, Yang Y, Ding Y, et al. Mo-doped $Pr_{0.6}Sr_{0.4}Fe_{0.8}Ni_{0.2}O_{3-\delta}$ as potential electrodes for intermediate-temperature symmetrical solid oxide fuel cells. *Electrochim Acta*. 2017;227:33-40.
73. Burnwal SK, Bharadwaj S, Kistaiah P. Review on MIEC cathode materials for solid oxide fuel cells. *J Mol Eng Mater*. 2016;04(02):1630001.
74. Kim J, Sengodan S, Kwon G, et al. Triple-conducting layered perovskites as cathode materials for proton-conducting solid oxide fuel cells. *ChemSusChem*. 2014;7(10):2811-2815.
75. Fan L, Su P-C. Layer-structured $LiNi_{0.8}Co_{0.2}O_2$: a new triple $(H^+/O^{2-}/e^-)$ conducting cathode for low temperature proton conducting solid oxide fuel cells. *J Power Sources*. 2016;306:369-377.
76. Song Y, Chen Y, Wang W, et al. Self-assembled triple-conducting nanocomposite as a superior protonic ceramic fuel cell cathode. *Joule*. 2019;3(11):2842-2853.
77. Zhang W, Hu YH. Progress in proton-conducting oxides as electrolytes for low-temperature solid oxide fuel cells: from materials to devices. *Energy Sci Eng*. 2021;9(7):984-1011.
78. Tao Z, Fu M, Liu Y, et al. High-performing proton-conducting solid oxide fuel cells with triple-conducting cathode of $Pr_{0.5}Ba_{0.5}(Co_{0.7}Fe_{0.3})O_{3-\delta}$ tailored with W. *Int J Hydrogen Energy*. 2022;47(3):1947-1953.
79. Sun C, Hui R, Roller J. Cathode materials for solid oxide fuel cells: a review. *J Solid State Electrochem*. 2010;14(7):1125-1144.
80. Istomin SY, Antipov EV. Cathode materials based on perovskite-like transition metal oxides for intermediate temperature solid oxide fuel cells. *Russ Chem Rev*. 2013;82(7):686-700.
81. Huang Y, Vohs JM, Gorte RJ. Fabrication of Sr-doped $LaFeO_3$ YSZ composite cathodes. *J Electrochem Soc*. 2004;151(4):A646.
82. Chiba R. An investigation of $LaNi_{1-x}Fe_xO_3$ as a cathode material for solid oxide fuel cells. *Solid State Ionics*. 1999;124(3-4):281-288.
83. Goodenough JB. Oxide-ion conductors by design. *Nature*. 2000;404(6780):821-823.
84. Vágner P, Guhlke C, Miloš V, Müller R, Fuhrmann J. A continuum model for yttria-stabilized zirconia incorporating triple phase boundary, lattice structure and immobile oxide ions. *J Solid State Electrochem*. 2019;23:2907-2926.
85. Chen XJ, Khor KA, Chan SH, Yu LG. Influence of microstructure on the ionic conductivity of yttria-stabilized zirconia electrolyte. *Mater Sci Eng A*. 2002;335(1-2):246-252.
86. Joo J, Choi G. Electrical conductivity of YSZ film grown by pulsed laser deposition. *Solid State Ionics*. 2006;177(11-12):1053-1057.
87. Wang B, Zhu B, Yun S, et al. Fast ionic conduction in semiconductor $CeO_{2-\delta}$ electrolyte fuel cells. *NPG Asia Mater*. 2019;11(1):51.
88. Ishihara T, Matsuda H, Takita Y. Doped $LaGaO_3$ perovskite type oxide as a new oxide ionic conductor. *J Am Chem Soc*. 1994;116(9):3801-3803.
89. Huang K, Tichy RS, Goodenough JB. Superior perovskite oxide-ion conductor; strontium- and magnesium-doped $LaGaO_3$: I, phase relationships and electrical properties. *J Am Ceram Soc*. 1998;81(10):2565-2575.
90. Huang K, Wan J-H, Goodenough JB. Increasing power density of LSGM-based solid oxide fuel cells using new anode materials. *J Electrochem Soc*. 2001;148(7):A788.
91. Matraszek A. Phase diagram study in the La_2O_3–Ga_2O_3–MgO–SrO system in air. *Solid State Ionics*. 2004;166(3-4):343-350.
92. Ding H, Tao Z, Liu S, Yang Y. A redox-stable direct-methane solid oxide fuel cell (SOFC) with $Sr_2FeNb_{0.2}Mo_{0.8}O_{6-\delta}$ double perovskite as anode material. *J Power Sources*. 2016;327:573-579.
93. Sciazko A, Komatsu Y, Yokoi R, Shimura T, Shikazono N. Effects of mass fraction of $La_{0.9}Sr_{0.1}Cr_{0.5}Mn_{0.5}O_{3-\delta}$ and $Gd_{0.1}Ce_{0.9}O_{2-\delta}$ composite anodes for nickel free solid oxide fuel cells. *J Eur Ceram Soc*. 2022;42(4):1556-1567.
94. Yan J, Matsumoto H, Enoki M, Ishihara T. High-power SOFC using $La_{0.9}Sr_{0.1}Ga_{0.8}Mg_{0.2}O_{3-\delta}/Ce_{0.8}Sm_{0.2}O_{2-\delta}$ composite film. *Electrochem Solid State Lett*. 2005;8(8):A389.
95. Wachsman ED, Lee KT. Lowering the temperature of solid oxide fuel cells. *Science*. 2011;334(6058):935-939.
96. Fan L, Zhu B, Su P-C, He C. Nanomaterials and technologies for low temperature solid oxide fuel cells: recent advances, challenges and opportunities. *Nano Energy*. 2018;45:148-176.
97. Hua D, Li G, Lu H, Zhang X, Fan P. Investigation of carbon formation on Ni/YSZ anode of solid oxide fuel cell from CO

disproportionation reaction. *Int Commun Heat Mass Transfer*. 2018;91:23-29.
98. Huang K, Goodenough JB. A solid oxide fuel cell based on Sr- and Mg-doped $LaGaO_3$ electrolyte: the role of a rare-earth oxide buffer. *J Alloys Compd*. 2000;303-304:454-464.
99. Leng Y, Chan S, Jiang S, Khor K. Low-temperature SOFC with thin film GDC electrolyte prepared in situ by solid-state reaction. *Solid State Ionics*. 2004;170(1-2):9-15.
100. Han M, Tang X, Yin H, Peng S. Fabrication, microstructure and properties of a YSZ electrolyte for SOFCs. *J Power Sources*. 2007;165(2):757-763.
101. Finnerty CM, Coe NJ, Cunningham RH, Ormerod RM. Carbon formation on and deactivation of nickel-based/zirconia anodes in solid oxide fuel cells running on methane. *Catal Today*. 1998;46(2-3):137-145.
102. Sun C, Su R, Chen J, Lu L, Guan P. Carbon formation mechanism of C_2H_2 in Ni-based catalysts revealed by in situ electron microscopy and molecular dynamics simulations. *ACS Omega*. 2019;4(5):8413-8420.
103. Sun C, Stimming U. Recent anode advances in solid oxide fuel cells. *J Power Sources*. 2007;171(2):247-260.
104. Yang Q, Chai F, Ma C, Sun C, Shi S, Chen L. Enhanced coking tolerance of a MgO-modified Ni cermet anode for hydrocarbon fueled solid oxide fuel cells. *J Mater Chem A*. 2016;4(46):18031-18036.
105. Yang Q, Chen J, Sun C, Chen L. Direct operation of methane fueled solid oxide fuel cells with Ni cermet anode via Sn modification. *Int J Hydrogen Energy*. 2016;41(26):11391-11398.
106. Zhang W, Wei J, Yin F, Sun C. Recent advances in carbon-resistant anodes for solid oxide fuel cells. *Mater Chem Front*. 2023;7:1943-1991. doi:10.1039/D2QM01366E
107. Sumi H, Lee Y-H, Muroyama H, et al. Effect of carbon deposition by carbon monoxide disproportionation on electrochemical characteristics at low temperature operation for solid oxide fuel cells. *J Power Sources*. 2011;196(10):4451-4457.
108. Hu YH, Ruckenstein E. Temperature-programmed desorption of CO adsorbed on NiO/MgO. *J Catal*. 1996;163(2):306-311.
109. Hu YH, Ruckenstein E. Comment on "Dry reforming of methane by stable Ni–Mo nanocatalysts on single-crystalline MgO". *Science*. 2020;368(6492):eabb5459.
110. Kim H, Lu C, Worrell WL, Vohs JM, Gorte RJ. Cu-Ni cermet anodes for direct oxidation of methane in solid-oxide fuel cells. *J Electrochem Soc*. 2002;149(3):A247.
111. Wu L, Wang S, Wang S, Xia C. Enhancing the performance of doped ceria interlayer for tubular solid oxide fuel cells. *J Power Sources*. 2013;240:241-244.
112. Khan MZ, Song R-H, Mehran MT, Lee S-B, Lim T-H. Controlling cation migration and inter-diffusion across cathode/interlayer/electrolyte interfaces of solid oxide fuel cells: a review. *Ceram Int*. 2021;47(5):5839-5869.
113. Zhang L, Chen G, Dai R, Lv X, Yang D, Geng S. A review of the chemical compatibility between oxide electrodes and electrolytes in solid oxide fuel cells. *J Power Sources*. 2021;492:229630.

How to cite this article: Zhang W, Hu YH. Material design and performance of carbon monoxide-fueled solid oxide fuel cells: a review. *Energy Sci Eng*. 2023;1-13. doi:10.1002/ese3.1502